
FLuID: Mitigating Stragglers in Federated Learning using Invariant Dropout

Irene Wang

University of British Columbia
iwang05@student.ubc.ca

Prashant Nair

University of British Columbia
prashantnair@ece.ubc.ca

Divya Mahajan

Microsoft
divya.mahajan@microsoft.com

Abstract

Federated Learning (FL) allows machine learning models to train locally on individual mobile devices, synchronizing model updates via a shared server. This approach safeguards user privacy; however, it also generates a heterogeneous training environment due to the varying performance capabilities across devices. As a result, “straggler” devices with lower performance often dictate the overall training time in FL. In this work, we aim to alleviate this performance bottleneck due to stragglers by dynamically balancing the training load across the system. We introduce *Invariant Dropout*, a method that extracts a sub-model based on the weight update threshold, thereby minimizing potential impacts on accuracy. Building on this dropout technique, we develop an adaptive training framework, Federated Learning using Invariant Dropout (FLuID). FLuID offers a lightweight sub-model extraction to regulate computational intensity, thereby reducing the load on straggler devices without affecting model quality. Our method leverages neuron updates from non-straggler devices to construct a tailored sub-model for each straggler based on client performance profiling. Furthermore, FLuID can dynamically adapt to changes in stragglers as runtime conditions shift. We evaluate FLuID using five real-world mobile clients. The evaluations show that Invariant Dropout maintains baseline model efficiency while alleviating the performance bottleneck of stragglers through a dynamic, runtime approach.

1 Introduction

Federated Learning (FL) enables machine learning models to train on edge and mobile devices, synchronizing the model updates via a common server [SB09, SVHN10, LSTS20, ZBW⁺22]. This method ensures user privacy as local data remains on the device, obviating the need for storing it in the cloud [MMR⁺17]. However, FL introduces heterogeneity due to varying performance capabilities of the devices. Consequently, straggler devices with lower computational and network performance often dictate training latency and throughput, as shown in Figure 1.

Previous research attempts to mitigate the impact of stragglers through asynchronous aggregation, where clients update the server model independently and asynchronously [CCA⁺21, CNSR20, XKG19]. While this approach alleviates some of the detrimental effects of stragglers, it can introduce staleness into the global model, potentially leading to slower convergence and lower accuracy [BHS20, CCA⁺21, WUH⁺21, HBGS19].

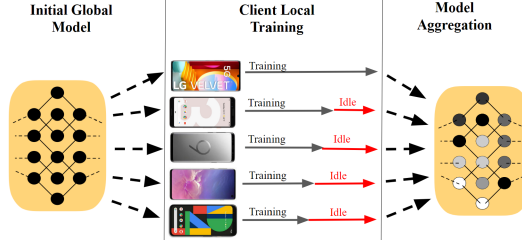


Figure 1: Straggler’s impact on FL performance. In synchronous FL, all clients wait for the straggler for global model aggregation.

Other research proposes eliminating updates from slower devices entirely. [KMA⁺19]. However, this approach can introduce training bias, as it effectively excludes certain clients and their respective data. To ensure the contribution of all devices, recent works in this area employ a dropout technique where the stragglers only train a subset of the global model [HLA⁺21, MGZP22]. The overall accuracy of the model is determined by the subset of neurons that are dropped from the global model. Thus, previous work alleviates the training load on stragglers by either incurring training bias, creating performance-centric sub-models, or entirely reconstructing the sub-model.

Our paper proposes a novel dropout technique called Invariant Dropout, which identifies "invariant" neurons—those that train quickly and show little variation during training. We observe that the training (computational load) and transfer (communication load) of these invariant neurons to and from the straggler devices contribute minimally to the efficiency of the global model. Thus, they can be dropped. We observe that after only 30% of the training iterations, 15%-30% of the neurons become invariant across CIFAR10 [Kri09], and LEAF datasets FEMNIST, and Shakespeare [CDW⁺18]. We observe that the training (computational load) and transfer (communication load) of these invariant neurons to and from the straggler devices contribute minimally to the efficiency of the global model. Thus, they can be dropped. Building on this insight, we develop a dynamic framework called Federated Learning using Invariant Dropout (FLuID), which adjusts the sub-model size based on both the magnitude of neuron updates and the computational capabilities of the client devices. In addition to introducing a new dropout technique, unlike prior work, FLuID periodically calibrates the sub-model size during runtime to account for changes in stragglers due to factors like low battery or network issues.

Overall, we face two challenges in building FLuID- identifying invariant neurons and establishing a dynamic lightweight method for straggler identification and sub-model size determination at runtime. FLuID addresses the first challenge by leveraging the non-straggler clients, which typically outnumber stragglers, to identify invariant neurons. The server is not used for this purpose as it receives updates from stragglers running a sub-model. For the second challenge, FLuID uses a drop-threshold, below which neurons are dropped, allowing dynamic sub-model determination for each straggler. By profiling client training times and identifying stragglers during the initial epochs of each calibration step, FLuID can incrementally adjust the drop-threshold until the number of selected neurons matches the target sub-model size for stragglers.

Our evaluation of FLuID on various models, datasets, and real-world mobile devices shows an up to 18% speedup in performance. Additionally, it improves training accuracy by a maximum of 1.4 percentage points over the state-of-the-art Ordered Dropout, all while mitigating the computational performance overheads caused by straggler devices.

2 Related Work

In the domain of heterogeneous client optimization, several prior work have tried to mitigate the effects of stragglers.

Dropout techniques. Federated Dropout [CKMT18, RKPH22] randomly drops portions of the global model, sending a sub-model to the slower devices. However, this may potentially impact accuracy. Subsequent work, Ordered Dropout [HLA⁺21, DDT21], mitigates this accuracy loss by regulating which neurons are dropped, either from the left or right portions of the global model. Other methods, such as those outlined in [MGZP22], use a low-rank approximation to identify over-parameterized

neurons and generate tailored sub-models. Despite these advancements, none of these works consider the individual contribution of each neuron while creating a sub-model. In contrast, our work not only introduces a novel dropout technique that takes into account the contribution of each neuron but also provides a framework capable of dynamically identifying slower devices and adjusting the dropout rate accordingly.

Server offloading strategies using split learning. The approach proposed by [WUH⁺21] employs split learning to offload part of the model to the server, while [HAA20] transfers their knowledge to a larger server-side CNN. [UWH⁺21] focuses on device mobility during Federated Learning, offloading training to edge servers. Finally, [WQR⁺22] introduces a compression method for split learning. However, unlike these methods, Invariant Dropout does not require data transfer out of the device and into the server, instead conducts all training on client devices. Nonetheless, if data movement is a possibility, Invariant Dropout can be stacked on top of these techniques to determine which part of the model needs to be offloaded to the server.

Communication Optimizations. To reduce learning time, [HWL20] proposes an online learning algorithm that determines sparsity based on communication and computational capabilities. [CSP⁺21] introduces a Federated Learning framework utilizing a probabilistic device selection method and quantization to lessen communication overhead. [XFD⁺21] proposes a framework featuring overhead reduction techniques for efficient training on resource-limited edge devices, including pruning and quantization. Unlike these works, Invariant Dropout avoids both communication and computation overhead by dropping the least contributing "invariant" neurons, presenting a new insight compared to these prior works.

Model Pruning. PruneFL [JWK⁺22] introduces an approach to dynamically select model sizes during FL and reduce communication and computation overhead, thereby minimizing training time. Work in [MSA⁺21] prunes the global model for slower clients by excluding neurons with no or small activations. These approaches either generate a single sub-model for all clients, including non-stragglers, to train on or generate a static sub-model for the entire training process which can result in the stragglers permanently losing the opportunity to contribute to certain parts of the model. In contrast, Invariant Dropout enables the generation of multiple sub-models with various resource budgets and dynamically chooses a sub-model for each round based on current neuron contribution.

Coded Federated Learning. CodedPaddedFL and CodedSecAgg [SKRA21] utilize coding strategies to mitigate the impact of slower devices. CodedPaddedFL combines one-time padding with gradient codes to yield resiliency against stragglers. CodedSecAgg, based on Shamir’s secret sharing, allows clients to share an encoded version of their data with other devices. Unlike these methods, Invariant Dropout allows each client to keep their data locally.

3 Background and Motivation

3.1 Challenges in Federated Learning

In FL’s synchronous aggregation protocols [CCA⁺21], the server hosts a global model and regularly aggregates updates from clients, which are then redistributed to clients. Thus, system heterogeneity remains a significant challenge in FL [DTS⁺22, LSTS20]. As shown in Figure 2a, we observe significant differences in training times across five mobile devices engaged in Federated Learning without any dropout mechanism in place. Depending on the dataset and machine learning model, training time can vary significantly, with differences of up to twofold across datasets such as CIFAR10, FEMNIST, and Shakespeare. We find that any client can become a straggler, regardless of the dataset or machine learning model in use. Furthermore, the performance of mobile devices in Federated Learning can fluctuate over time due to varying network bandwidth and resource availability. In Section 6.1 and Figure 4b, we provide a more detailed discussion on how stragglers change over time. In response to these observations, we develop FLUID, a system designed to dynamically identify stragglers and adjust the training load to balance performance with non-straggler devices.

3.2 Dropout Techniques

Model dropout is a technique that involves sending a subset of the global model, known as a sub-model, to stragglers for load balancing. There are two state-of-the-art proposals in this space:

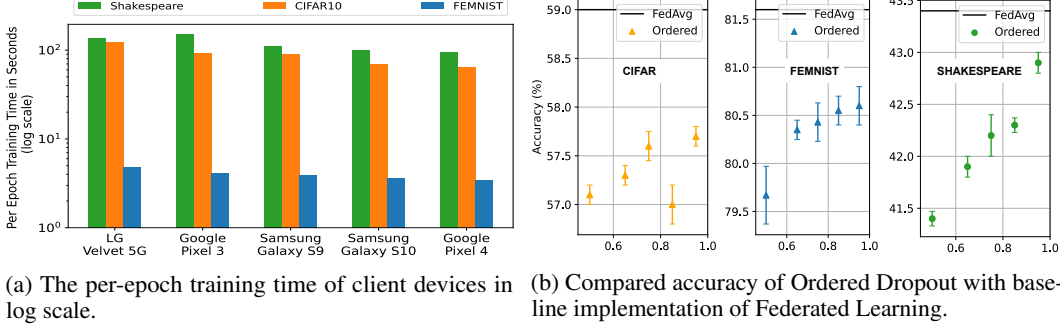


Figure 2: (a) Performance variation across mobile devices (in log scale), (b) accuracy implications of prior dropout (static) techniques.

Federated Dropout [CKMT18] and Ordered Dropout from FjORD [HLA⁺21]. Federated Dropout randomly drops neurons, simplifying the selection of sub-models, but reducing the global model’s accuracy. In contrast, Ordered Dropout systematically drops neurons by maintaining order within the sub-model. These works demonstrate that the sub-model’s neuron selection is crucial for the global model’s accuracy. In the context of this work, "neurons" refer to filters in convolutional (CONV) layers, activations in fully-connected (FC) layers, and hidden units in Long Short-Term Memory (LSTM) [HS97] layers.

Accuracy Implications with dropout: Figure 2b compares the testing accuracy of a non-dropout vanilla Federated Learning (FL) implementation with Ordered Dropout. This comparison is performed using five mobile devices, one of which is a straggler, across three different datasets: CIFAR10 [Kri09], FEMNIST, and Shakespeare [CDW⁺18]. As the sub-model size decreases, we observe that across all three datasets and machine learning models, Ordered Dropout experiences up to a 2.5 percentage point drop in accuracy. We vary the sub-model size from 0.5 (representing 50% of the global model) to 1 (the entire model). The results with 50-100 clients and 20% of them being stragglers are provided in Section 6.1.

4 Invariant Dropout

Invariant Dropout enables stragglers to only train on a sub-model consisting of neurons that ‘vary’ over time and contribute to the global model. Invariant dropout achieves this by selecting a subset (i) of sub-models (s_i) from a total sub-model distribution (S), where each sub-model represents a different number of neurons and thus varies in compute and memory requirements. Appendix A.1 illustrates this temporal variation across several neurons in the evaluated models. Note that all clients including the straggler still perform inference on the full model.

4.1 Proposed dropout mechanism

Invariant Dropout selects a sub-model from a set of sub-models, S , composed of m total sub-models, denoted as $S = s_1, s_2, \dots, s_m$. Each sub-model s_i contains neuron layers a_1, a_2, \dots, a_k . The size of the sub-model corresponds to a dropout rate r that is based on the drop-threshold th for the dropout mechanism. Given a change in neuron value, $g = \Delta a$, we can select the sub-model $s_i = \{a_1, a_2, \dots, a_k\}$ where the updates in neurons within the sub-model satisfy $g \geq th \forall a_j \in s_i$ and $1 \leq j \leq k$. FLuID, which we describe below, selects s_i such that the compute utilization and memory footprint can effectively mitigate the inefficiency of the straggler.

Next, we assume that the system includes C clients with T stragglers and N non-stragglers. T and N are exclusive and independent subsets of C , where $T \cup N = C$ and $T \cap N = \phi$. Invariant Dropout maintains a dropout rate $r \in (0, 1]$ per layer across the T stragglers. However, the complexity of selecting $a_j(t+1)$ will vary with each sub-model s_i . To reduce the computational overhead of selecting the appropriate sub-model, ID leverages non-straggler clients to provide directions on the set of $a_j(t+1)$. The server computes over a subset of potential sub-models s_i to select the one with the maximum updates to the neurons.

4.2 Variance in Gradients with Invariant Dropout

Consider C clients participating in Federated Learning. The training data is represented as $x_c c = 1^C$, where c denotes one client, and each client has a corresponding loss function $f_{c=1}^C$. Learning minimizes the loss function using the following optimization: $f(w) := \frac{1}{C} \sum_{c=1}^C f_c(w)$, where $w_{t+1} = w_t - \eta_t(g(w_t))$.

Invariant Dropout can be viewed as a sparse stochastic gradient vector, where each gradient has a certain probability of being dropped. The gradient vector is denoted as $G = [g_1, g_2, \dots, g_k]$ where $g \in R$ and each gradient has a probability of being retained and transmitted across the network, represented as $[p_1, p_2, \dots, p_k]$. The sparse vector for the stragglers is represented as G_s . The variance of the ID-based gradient vector can be represented as $E(G_s^2) = \sum_{i=1}^k (g_i^2 p_i)$ [WWLZ18, XYXC21]. The variance of the dropout vector is a small factor deviation from the non-dropout gradient vector represented as follows:

$$\min \sum_{i=1}^k p_i : \sum_{i=1}^k (g_i^2 p_i) = (1 + \epsilon) \sum_{i=1}^k g_i^2 \quad (1)$$

Invariant Dropout drops weights based on the $g = \Delta a$ gradient across epochs. Thus, weights with higher gradient values have a lower probability of being dropped. This implies if $|g_i| > |g_j|$ then $p_i > p_j$. The probability of a gradient not getting dropped (p_i) is inversely proportional to the dropout rate r . Let's assume that the top- k magnitude of gradient values are not dropped. Hence if $G = [g_1, g_2, \dots, g_m]$ is assumed to be sorted, then $G = [g_1, g_2, \dots, g_k]$ has a $p = 1$, whereas the $G = [g_{k+1}, g_{k+2}, \dots, g_d]$ have a probability of $p_i = \frac{|g_i|}{r}$. This modifies the optimization problem in Equation 1 to:

$$\sum_{i=1}^k g_i^2 + \sum_{i=k+1}^m \frac{|g_i|}{r} - (1 + \epsilon) \sum_{i=1}^m g_i^2 = 0, \frac{|g_i|}{r} \leq 1 \quad (2)$$

Which implies that

$$r = \frac{\sum_{i=k+1}^m |g_i|}{(1 + \epsilon) \sum_{i=1}^m g_i^2 - \sum_{i=1}^k g_i^2} \quad (3)$$

As per the constraint $\frac{|g_i|}{r} \leq 1$:

$$|g_i| \left(\sum_{i=k+1}^m |g_i| \right) \leq (1 + \epsilon) \sum_{i=1}^m g_i^2 - \sum_{i=1}^k g_i^2 \quad (4)$$

Invariant Dropout retains the gradients with the greatest magnitude. As a result, the boundedness of the expected value from Equation 1 can be represented as follows:

$$\sum_{i=1}^m p_i = \sum_{i=1}^k p_i + \sum_{i=k+1}^m p_i \quad (5)$$

$$\sum_{i=1}^m p_i = k + |g_i| \sum_{i=k+1}^m \left(\frac{\sum_{i=k+1}^m |g_i|}{(1 + \epsilon) \sum_{i=1}^m g_i^2 - \sum_{i=1}^k g_i^2} \right) \quad (6)$$

$$\sum_{i=1}^m p_i \leq k(1 + \epsilon) \quad (7)$$

As such, the variance of the gradient in ID is bounded by Equation 7.

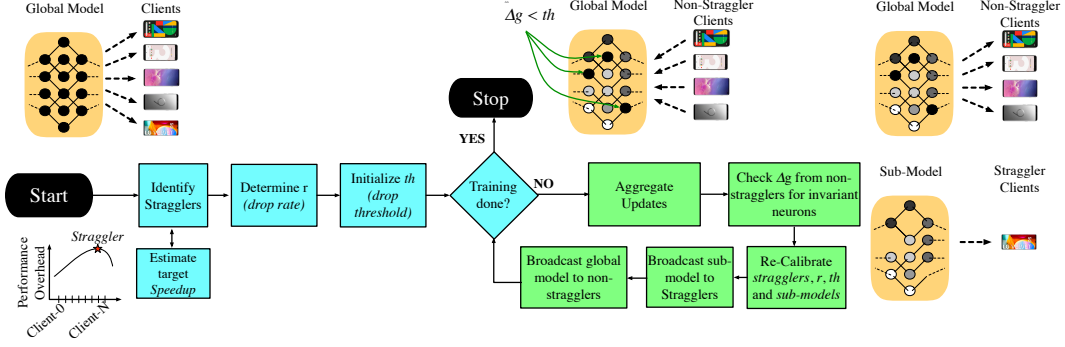


Figure 3: The workflow of FLuID. The non-stragglers are used to determine the neurons that are not updated within a set threshold. Thereafter, sub-models are dynamically created by dropping invariant neurons. These sub-models are sent to the straggler devices.

5 FLuID Framework

Figure 3 shows the flow of Federated Learning using Invariant Dropout (FLuID). In FLuID, each calibration step includes straggler determination (T), discovering invariant neurons (IN) and drop threshold (th), and sub-model extraction (s_i). Currently, the calibration occurs per epoch, which refers to one training run over the complete client dataset. However, the frequency of calibration can be reduced if the invariant neurons and stragglers do not significantly change over steps since FLuID does incur a low overhead.

Algorithm 1 outlines the FLuID framework. At the onset of Federated Learning, FLuID identifies the stragglers. To achieve this, FLuID runs the global model on all clients, including stragglers, and measures the performance delay between the slowest client’s training time ($T_{straggler}$) and the target training time (T_{target}). T_{target} is set equal to the training time of the ‘next slowest client’. The required speedup for stragglers is calculated as $Speedup = \frac{T_{straggler}}{T_{target}}$. This speedup ensures optimal utilization of available clients. The initial calibration is carried out in lines 7-11 and 21-25 of the algorithm. Note, it takes a few epochs to calibrate the initial threshold, stragglers, and submodel. In subsequent calibration steps, the global server continues to measure the training time of clients and thereby identifies if there is any change in the straggler cohort.

Tuning the Performance of Stragglers. The sub-model size is determined by calculating the dropout rate r as detailed in lines 21-24 of Algorithm 1. The value of r is selected to ensure that the updated straggler training time, denoted as $T_{straggler_{new}}$, is close to the target training time (T_{target}). To do so, FLuID chooses an r that is closest to the inverse of the speedup. Figure 7 in the Appendix demonstrates a linear relationship between a client’s training time and the sub-model size.

Determining the Drop Threshold at Runtime Once FLuID has identified the stragglers and the dropout rate, it iteratively adjusts the threshold to drop as many invariant neurons as possible. Appendix A.2 discusses the importance of choosing a threshold on the performance. Lets assume $w_{ijc}(t)$ represents the set of weights of the i th neuron in the j th layer for client c after the training epoch t . The percent difference g of the neuron, for each client c , is the minimum value of g as denoted by: $g \geq \frac{w_{ijc}(t) - w_{ijc}(t-1)}{w_{ijc}(t-1)}$. Neurons that are potential candidates for dropping are those whose weight updates are within the threshold (th) compared to the previous calibration point. Unfortunately, determining the appropriate th poses a few challenges.

In order to identify neuron drop candidates, the global server cannot rely on updates from all clients since stragglers only train on and update the sub-model. Instead, the server takes advantage of the fact that non-stragglers train on the complete model and can identify neurons whose weight updates fall within the threshold (th) for each calibration step. FLuID prioritizes dropping neurons on stragglers whose weight updates fall within the threshold (th) for the majority of non-stragglers.

The initial threshold value (th) in the FLuID framework is set as the average of the minimum percent update of all neurons in the initial few training epochs. The threshold is incrementally increased after each epoch until the number of neurons below the threshold is greater than or equal to the number of

Algorithm 1 FLuID executing on Centralized Server

```
1: Input:  $M(w)$  # Model.  $M(w_t)$  is model at step  $t$ 
2: Output:  $S(w)$  # Sub-models for stragglers
3:  $N \rightarrow$  All Clients,  $T \rightarrow \emptyset$  #  $T$  stragglers,  $N$  non-stragglers
4:  $IN \rightarrow \emptyset$  # invariant neurons
5: while not done do
6:   if  $T$  is  $\emptyset$  then {# Straggler and dropout threshold initialization}
7:     Broadcast  $M(w_0)$  to each  $C$ 
8:     Receive  $M(w_1)$  from every  $C$ 
9:      $th = \min(\frac{w_{ijct} - w_{ij(t-1)}}{w_{ij(t-1)}})$  # threshold for Invariant dropout
10:   else {# Straggler and dropout threshold recalibration}
11:      $S(w_t) = \text{sub\_model\_generation}(inv, M(w_t))$ 
12:     Broadcast  $S(w_t)$  all  $i \in T$ 
13:     Broadcast  $M(w_t)$  all  $i \wedge i \notin T$ 
14:     Receive  $\Delta(w_{t+1})$  from every  $C$ 
15:      $M(w_{t+1}) = \text{aggregate}(M(w_t), \Delta(w_{t+1}))$ 
16:      $IN = \text{identify\_invariant\_neurons}(th, \Delta(w_{t+1}), N)$ 
17:   end if
18:    $T, N, L = \text{determine\_stragglers}(C)$  #  $L$  = train latencies
19:    $T_{target} = \text{identify\_next\_slowest\_client}(L)$ 
20:    $Speedup_i = \frac{T_{straggler_i}}{T_{target}}$ 
21:    $r_i, S_i = \text{calculate\_submodel\_size}(Speedup_i)$  #  $r_i$  dropout rate
22:    $th = \text{increment\_threshold}(r_i)$ 
23:   done = check\_training\_done( $M(w_t)$ )
24: end while
```

neurons to be left out of the sub-model. FLuID can have a different drop threshold for each layer. The algorithm targets neurons for dropping whose gradients consistently fall below the threshold over multiple epochs, prioritizing the elimination of non-critical neurons.

This entire process is repeated to recalibrate the stragglers, the drop rate (r), and the threshold (th).

6 Evaluation Setup

Models and datasets. We evaluate FLuID on three models and datasets [MGZP22, HLA⁺21].

The FEMNIST datasets consist of images of numbers and letters, partitioned based on the writer of the character in non-IID setting. We train a CNN with two 5x5 CONV layers with 16 and 64 channels respectively, each of them followed with 2x2 max-pooling. The model also includes a fully connected dense layer with 120 units and a softmax output layer. The model is trained using a batch size of 10 and a learning rate of 0.004.

The Shakespeare dataset partitions data based on roles in Shakespeares' plays in non-IID setting. We train a two-layer LSTM classifier containing 128 hidden units. We train the model with a batch size of 128 and a learning rate of 0.001.

The CIFAR10 dataset consists of images, partitioned using the same strategy as FjORD [HLA⁺21] and used the IID partition provided by the Flower [BTM⁺20]. We train a VGG-9 [SZ15] architecture model with 6 3x3 CONV layers (the first 2 have 32 channels, followed by two 64-channel layers, and lastly two 128-channel layers), two FC dense layers with 512 and 256 units and a final softmax output layer. We train the model with a batch size of 20 and a learning rate of 0.01. For the evaluation on real-world mobile devices, we selected the VGG-9 model due to its ability to fit within the resource constraints of all the mobile phones we tested. The model also executed within a reasonable timeframe without crashing. We conduct scalability experiments using the ResNet-18 model, and the results are presented in section 6.1 and Figure 5b. It is worth noting that we evaluated all the baseline dropout methods and Invariant Dropout using the same setup.

System Configuration. Table 1 provides the details of the phones used for the experiments. We evaluate five clients and identify one straggler per training epoch. We connect all our client devices

and our server over the same network. All the clients run on Android mobile phones from the years 2018 to 2020.

FLuID is implemented on top of the Flower (v0.18.0) [BTM⁺20] framework and TensorFlow Lite [Goo] from TensorFlow v2.8.0 [ABC⁺16]. Models are defined using TensorFlow’s Sequential API, and then converted into .tflite formats.

Table 1: Software-Hardware specifications of clients

Device	Year	Android Version	CPU (Cores)
LG Velvet 5G	2020	10	1×2.4 GHz Kryo 475 Prime + 1×2.2 GHz Kryo 475 Gold + 6×1.8 GHz Kryo 475 Silver
Google Pixel 3	2018	9	4×2.5 GHz Kryo 385 Gold + 4×1.6 GHz Kryo 385 Silver
Samsung Galaxy S9	2018	10	4×2.8 GHz Kryo 385 Gold + 4×1.7 GHz Kryo 385 Silver
Samsung Galaxy S10	2019	11	2×2.73 GHz Mongoose M4 + 2×2.31 GHz Cortex-A75 + 4×1.95 GHz Cortex-A55
Google Pixel 4	2019	12	1×2.84 GHz Kryo 485 + 3×2.42 GHz Kryo 485 + 4×1.78 GHz Kryo 485

Table 2: Accuracy comparison of Random Dropout, Ordered Dropout, and Invariant Dropout. The text in **bold** indicates instances when Invariant Dropout showcases the highest accuracy. (μ = mean, σ = standard deviation, and r = sub-model as a fraction of global model).

Dataset	Dropout Method	$r = 0.95$		$r = 0.85$		$r = 0.75$		$r = 0.65$		$r = 0.5$	
		Accuracy (μ)	σ	Accuracy (μ)	σ	Accuracy (μ)	σ	Accuracy (μ)	σ	Accuracy (μ)	σ
FEMNIST	Random	80.6	0.1	80.5	0.2	80.3	0.2	79.3	0.5	79.2	0.3
	Ordered	80.6	0.2	80.5	0.2	80.4	0.2	80.3	0.1	79.7	0.3
	Invariant	81.1	0.3	80.9	0.1	80.8	0.2	80.3	0.4	80.1	0.3
CIFAR10	Random	57.5	0.1	56.8	0.2	57.0	0.2	57.2	0.2	57.2	0.3
	Ordered	57.7	0.1	57.0	0.2	57.6	0.2	57.3	0.1	57.1	0.1
	Invariant	58.2	0.1	58.4	0.3	57.1	0.1	57.5	0.2	57.4	0.2
Shakespeare	Random	43.3	0.1	42.5	0.1	42.4	0.1	41.8	0.2	41.3	0.1
	Ordered	42.9	0.1	42.3	0.1	42.2	0.2	41.9	0.1	41.4	0.1
	Invariant	43.6	0.1	42.5	0.1	42.6	0.2	42.2	0.2	41.7	0.1

Evaluation metrics and baselines. We provide the average training performance (wall-clock time), accuracy, and standard deviations for all workloads and experiments. In each evaluation round, clients receive the global model and report their evaluation accuracy and loss on local data to the server. The server calculates the distributed accuracy and loss by performing a weighted average based on the number of testing examples for each client. We compare FLuID with two established baselines: 1) Random federated dropout [CKMT18] and 2) Ordered dropout from FjORD [HLA⁺21].

6.1 Results and Analysis

Accuracy Evaluation We conducted accuracy evaluations of Invariant Dropout, comparing it with two baselines, using different sub-model sizes. We trained the models for 100, 250, and 65 epochs for CIFAR10, FEMNIST, and Shakespeare datasets, respectively. Table 2 presents the average achieved accuracy (μ) along with the standard deviation (σ) for the three datasets. Specifically, invariant dropout outperforms Random Dropout across all three datasets. Compared to Random Dropout, our work achieves a maximum accuracy gain of 1.6% points and on average 0.7% point higher accuracy for FEMNIST, 0.6% point higher accuracy for CIFAR10, and 0.3% point higher accuracy for Shakespeare datasets.

Invariant dropout also achieves a higher accuracy against Ordered Dropout across all three datasets, with a maximum increase in accuracy of 1.4% and an average increase of 0.3% for FEMNIST, 0.4% for CIFAR10, and 0.4% for Shakespeare. Additionally, Invariant dropout shows less variation in accuracy between runs of the same sub-model size and across all sub-model sizes. The accuracy improvements of invariant dropout are statistically significant ($r < 0.05$). This is due to the fact that the mechanism of invariant dropout eliminates only invariant neurons, which after certain training epochs, have little impact on the final model efficiency.

Computational Performance Evaluation Figure 4a shows FLuID’s capability to select the sub-model effectively, resulting in a significant reduction in the straggler’s training time to almost match that of the next slowest client. In the absence of FLuID, the straggler’s training time is typically 10% to 32% longer than the target time. However, after applying FLuID, the straggler’s training time is within 10% of the target time. Furthermore, it is observed that the overall accuracy of the global model tends to be higher when stragglers train with larger sub-models. Consequently, FLuID selects the largest possible sub-model size that minimizes training time variance across clients. It

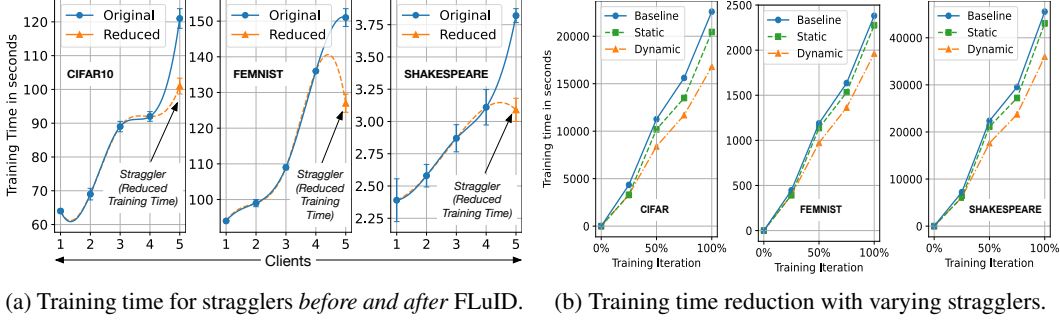


Figure 4: Performance evaluation of FLuID

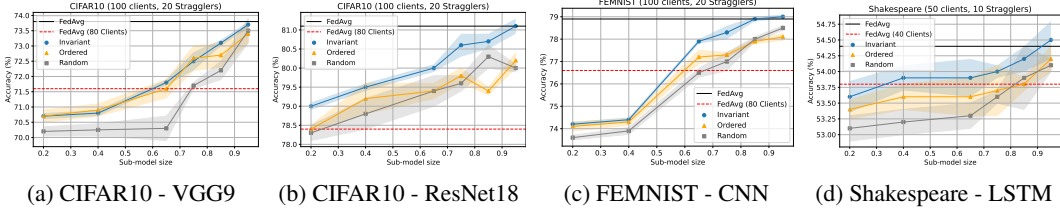


Figure 5: The accuracy comparison of Invariant Dropout with Ordered and Random Dropout as we scale to 50-100 clients with 20% of the slowest clients being stragglers.

is important to note that the performance improvement achieved through dropout is influenced by the size of the sub-model rather than the specific dropout technique employed. For a more detailed analysis of the impact of sub-model size on training time, please refer to Appendix A.3.

All results include the overhead of the FLuID framework, which, importantly, does not introduce a significant processing overhead to the overall training time. This is due to the fact that the additional computations required for threshold and sub-model calibration are performed centrally on the server, rather than being distributed to edge devices. We observe, FLuID calibration process takes significantly less time (less than 5%) compared to the actual training time.

Varying Stragglers at Runtime FLuID is capable of recalibrating stragglers, but during the experiments in Table 2, we observed that the performance of our mobile clients remained relatively stable in a steady state, without significant changes in the straggler. However, to evaluate the impact of varying conditions at runtime, we randomly executed certain clients at different points in the training process (25%, 50%, and 75% marks). This was achieved by enabling a client to run the training program as a background process between the specified periods. We observed that FLuID successfully adapted to the varying stragglers during runtime. Figure 4b demonstrates the overall training time for this experiment. On average, the FLuID framework achieved 18% to 26% faster training time compared to the baseline, and 14% to 18% faster training time compared to selecting a static straggler throughout the entire training process.

Scalability Studies To assess the scalability of invariant dropout, we conducted experiments using simulated clients ranging from 50 to 100. For the scalability tests each machine runs 10 to 20 clients in parallel. Among all clients, we identified the slowest 20% as stragglers. Figure 5 shows the accuracy performance across all three datasets. Overall, invariant dropout consistently outperforms Ordered and Random Dropout and maintains a better accuracy profile similar to Table 2. In addition, our dropout technique performs significantly better than completely excluding stragglers from the training process. We extended the experiment by clustering stragglers into multiple sub-model sizes in Appendix A.4. We also explore the impact of varying ratios of stragglers in Appendix A.5.

7 Limitations and Future Work

Although FLuID is able to mitigate some impact of the stragglers, it does incur minimal overhead to handle stragglers and maintain system performance. Our evaluation takes this into account but this overhead may increase if straggler performance constantly changes.

FLuID currently only uses pre-defined sub-model sizes mapped to straggler performance, which keeps the framework lightweight and avoids high overhead. However, for future works with varied edge devices, fine-grained sub-model determination may further enhance the work.

8 Conclusions

Due to rapid technological advancements and device variability in handheld devices, system heterogeneity is prevalent in federated learning. Straggler devices, which exhibit low computational performance, act as the bottleneck. In this paper, we address these issues by introducing a technique called Invariant Dropout. Invariant Dropout dynamically creates customized sub-models that include only the neurons exhibiting significant changes above a certain threshold. This approach effectively mitigates the performance overheads caused by stragglers while also achieving a higher accuracy compared to the state-of-the-art technique, Ordered Dropout.

References

- [ABC⁺16] Martín Abadi, Paul Barham, Jianmin Chen, Zhifeng Chen, Andy Davis, Jeffrey Dean, Matthieu Devin, Sanjay Ghemawat, Geoffrey Irving, Michael Isard, Manjunath Kudlur, Josh Levenberg, Rajat Monga, Sherry Moore, Derek G. Murray, Benoit Steiner, Paul Tucker, Vijay Vasudevan, Pete Warden, Martin Wicke, Yuan Yu, and Xiaoqiang Zheng. Tensorflow: A system for large-scale machine learning. In *Proceedings of the 12th USENIX Conference on Operating Systems Design and Implementation, OSDI’16*, page 265–283, USA, 2016. USENIX Association.
- [BHS20] Saar Barkai, Ido Hakimi, and Assaf Schuster. Gap-aware mitigation of gradient staleness. In *International Conference on Learning Representations*, 2020.
- [BTM⁺20] Daniel J. Beutel, Taner Topal, Akhil Mathur, Xinchu Qiu, Javier Fernandez-Marques, Yan Gao, Lorenzo Sani, Kwing Hei Li, Titouan Parcollet, Pedro Porto Buarque de Gusmão, and Nicholas D. Lane. Flower: A friendly federated learning research framework, 2020.
- [CCA⁺21] Zheng Chai, Yujing Chen, Ali Anwar, Liang Zhao, Yue Cheng, and Huzefa Rangwala. Fedat: A high-performance and communication-efficient federated learning system with asynchronous tiers. In *Proceedings of the International Conference for High Performance Computing, Networking, Storage and Analysis, SC ’21*, New York, NY, USA, 2021. Association for Computing Machinery.
- [CDW⁺18] Sebastian Caldas, Sai Meher Karthik Duddu, Peter Wu, Tian Li, Jakub Konečný, H. Brendan McMahan, Virginia Smith, and Ameet Talwalkar. Leaf: A benchmark for federated settings, 2018.
- [CKMT18] Sebastian Caldas, Jakub Konečný, H. Brendan McMahan, and Ameet Talwalkar. Expanding the reach of federated learning by reducing client resource requirements, 2018.
- [CNSR20] Yujing Chen, Yue Ning, Martin Slawski, and Huzefa Rangwala. Asynchronous online federated learning for edge devices with non-iid data. In *2020 IEEE International Conference on Big Data (Big Data)*, pages 15–24, 2020.
- [CSP⁺21] Mingzhe Chen, Nir Shlezinger, H. Vincent Poor, Yonina C. Eldar, and Shuguang Cui. Communication-efficient federated learning. *Proceedings of the National Academy of Sciences*, 118(17):e2024789118, 2021.
- [DDT21] Enmao Diao, Jie Ding, and Vahid Tarokh. Heteroff: Computation and communication efficient federated learning for heterogeneous clients. In *9th International Conference on Learning Representations, ICLR 2021, Virtual Event, Austria, May 3-7, 2021*. OpenReview.net, 2021.
- [DTS⁺22] Jie Ding, Eric Tramel, Anit Kumar Sahu, Shuang Wu, Salman Avestimehr, and Tao Zhang. Federated learning challenges and opportunities: An outlook, 2022.

- [Goo] Google. Tensorflow lite | ml for mobile and edge devices. <https://www.tensorflow.org/lite>. Accessed: 2022-08-14.
- [HAA20] Chaoyang He, Murali Annavaram, and Salman Avestimehr. Group knowledge transfer: Federated learning of large cnns at the edge. In H. Larochelle, M. Ranzato, R. Hadsell, M.F. Balcan, and H. Lin, editors, *Advances in Neural Information Processing Systems*, volume 33, pages 14068–14080. Curran Associates, Inc., 2020.
- [HBGS19] Ido Hakimi, Saar Barkai, Moshe Gabel, and Assaf Schuster. Taming momentum in a distributed asynchronous environment, 2019.
- [HLA⁺21] Samuel Horváth, Stefanos Laskaridis, Mario Almeida, Ilias Leontiadis, Stylianos Venieris, and Nicholas Donald Lane. FjORD: Fair and accurate federated learning under heterogeneous targets with ordered dropout. In A. Beygelzimer, Y. Dauphin, P. Liang, and J. Wortman Vaughan, editors, *Advances in Neural Information Processing Systems*, 2021.
- [HS97] Sepp Hochreiter and Jürgen Schmidhuber. Long short-term memory. *Neural computation*, 9(8):1735–1780, 1997.
- [HWL20] Pengchao Han, Shiqiang Wang, and Kin Kwong Leung. Adaptive gradient sparsification for efficient federated learning: An online learning approach. *2020 IEEE 40th International Conference on Distributed Computing Systems (ICDCS)*, pages 300–310, 2020.
- [JWK⁺22] Yang Jiang, Shiqiang Wang, Bongjun Ko, Wei-Han Lee, and Leandros Tassiulas. Model pruning enables efficient federated learning on edge devices. *IEEE transactions on neural networks and learning systems*, PP, 2022.
- [KMA⁺19] Peter Kairouz, H. Brendan McMahan, Brendan Avent, Aurélien Bellet, Mehdi Bennis, Arjun Nitin Bhagoji, Kallista A. Bonawitz, Zachary Charles, Graham Cormode, Rachel Cummings, Rafael G. L. D’Oliveira, Salim El Rouayheb, David Evans, Josh Gardner, Zachary Garrett, Adrià Gascón, Badi Ghazi, Phillip B. Gibbons, Marco Gruteser, Zaïd Harchaoui, Chaoyang He, Lie He, Zhouyuan Huo, Ben Hutchinson, Justin Hsu, Martin Jaggi, Tara Javidi, Gauri Joshi, Mikhail Khodak, Jakub Konečný, Aleksandra Korolova, Farinaz Koushanfar, Sanmi Koyejo, Tancrède Lepoint, Yang Liu, Prateek Mittal, Mehryar Mohri, Richard Nock, Ayfer Özgür, Rasmus Pagh, Mariana Raykova, Hang Qi, Daniel Ramage, Ramesh Raskar, Dawn Song, Weikang Song, Sebastian U. Stich, Ziteng Sun, Ananda Theertha Suresh, Florian Tramèr, Praneeth Vepakomma, Jianyu Wang, Li Xiong, Zheng Xu, Qiang Yang, Felix X. Yu, Han Yu, and Sen Zhao. Advances and open problems in federated learning. *CoRR*, abs/1912.04977, 2019.
- [Kri09] Alex Krizhevsky. Learning multiple layers of features from tiny images. 2009.
- [LSTS20] Tian Li, Anit Kumar Sahu, Ameet S. Talwalkar, and Virginia Smith. Federated learning: Challenges, methods, and future directions. *IEEE Signal Processing Magazine*, 37:50–60, 2020.
- [MGZP22] Yiqun Mei, Pengfei Guo, Mo Zhou, and Vishal Patel. Resource-adaptive federated learning with all-in-one neural composition. In *Advances in Neural Information Processing Systems*, 2022.
- [MMR⁺17] H. B. McMahan, Eider Moore, Daniel Ramage, Seth Hampson, and Blaise Agüera y Arcas. Communication-efficient learning of deep networks from decentralized data. In *AISTATS*, 2017.
- [MSA⁺21] Muhammad Tahir Munir, Muhammad Mustansar Saeed, Mahad Ali, Zafar Ayyub Qazi, and Ihsan Ayyub Qazi. Fedprune: Towards inclusive federated learning, 2021.
- [RKPH22] Martin Rapp, Ramin Khalili, Kilian Pfeiffer, and Jörg Henkel. Distreal: Distributed resource-aware learning in heterogeneous systems. In *Proceedings of the AAAI Conference on Artificial Intelligence*, volume 36, pages 8062–8071, 2022.

- [SB09] Venkatesh Shankar and Sridhar Balasubramanian. Mobile marketing: A synthesis and prognosis. *Journal of interactive marketing*, 23(2):118–129, 2009.
- [SKRA21] Reent Schlegel, Siddhartha Kumar, Eirik Rosnes, and Alexandre Graell i Amat. Cod-edpaddedfl and codedsecagg: Straggler mitigation and secure aggregation in federated learning, 2021.
- [SVHN10] Venkatesh Shankar, Alladi Venkatesh, Charles Hofacker, and Prasad Naik. Mobile marketing in the retailing environment: current insights and future research avenues. *Journal of interactive marketing*, 24(2):111–120, 2010.
- [SZ15] Karen Simonyan and Andrew Zisserman. Very deep convolutional networks for large-scale image recognition. In Yoshua Bengio and Yann LeCun, editors, *3rd International Conference on Learning Representations, ICLR 2015, San Diego, CA, USA, May 7-9, 2015, Conference Track Proceedings*, 2015.
- [UWH⁺21] Rehmat Ullah, Di Wu, Paul Harvey, Peter Kilpatrick, Ivor Spence, and Blesson Varghese. Fedfly: Towards migration in edge-based distributed federated learning, 2021.
- [WQR⁺22] Jianyu Wang, Hang Qi, Ankit Singh Rawat, Sashank Reddi, Sagar Waghmare, Felix X. Yu, and Gauri Joshi. Fedlite: A scalable approach for federated learning on resource-constrained clients, 2022.
- [WUH⁺21] Di Wu, Rehmat Ullah, Paul Harvey, Peter Kilpatrick, Ivor Spence, and Blesson Varghese. Fedadapt: Adaptive offloading for iot devices in federated learning, 2021.
- [WWLZ18] Jianqiao Wangni, Jialei Wang, Ji Liu, and Tong Zhang. Gradient sparsification for communication-efficient distributed optimization. In *NeurIPS*, 2018.
- [XFD⁺21] Wenyuan Xu, Weiwei Fang, Yi Ding, Meixia Zou, and Naixue N. Xiong. Accelerating federated learning for iot in big data analytics with pruning, quantization and selective updating. *IEEE Access*, 9:38457–38466, 2021.
- [XKG19] Cong Xie, Sanmi Koyejo, and Indranil Gupta. Asynchronous federated optimization, 2019.
- [XYXC21] Zirui Xu, Fuxun Yu, Jinjun Xiong, and Xiang Chen. Helios: Heterogeneity-aware federated learning with dynamically balanced collaboration. In *2021 58th ACM/IEEE Design Automation Conference (DAC)*, pages 997–1002, 2021.
- [ZBW⁺22] Zhengyi Zhong, Weidong Bao, Ji Wang, Xiaomin Zhu, and Xiongtao Zhang. Flee: A hierarchical federated learning framework for distributed deep neural network over cloud, edge and end device. *ACM Trans. Intell. Syst. Technol.*, jan 2022. Just Accepted.

A Appendix

A.1 Evolution of Invariant Neurons

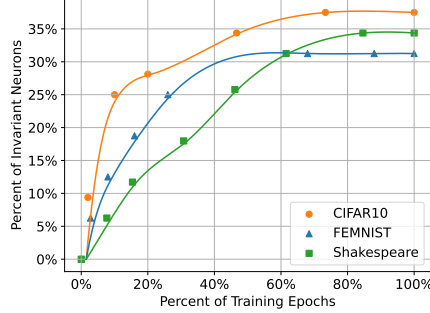


Figure 6: The percentage of ‘invariant’ neurons as the number of training rounds vary

In this section, we provide an example that some neurons in the server are trained quickly and vary only below a threshold in later iterations. Figure 6 shows the percentages of invariant neurons as the number of training epochs increases. Even after only 30% of the training rounds are completed, 15%-30% of the neurons become invariant across CIFAR10, FEMNIST, and Shakespeare datasets. For this example, we choose thresholds of 180%, 10%, and 500%, respectively, for these three datasets and compute their invariant neurons. Sending invariant neurons over to the straggler provides no utility; therefore, these neurons can be dropped. Our work FLuID builds upon this insight.

A.2 Choosing Suitable Threshold

Each model has different characteristics in terms of the magnitude of neuron updates. Therefore, choosing different threshold values results in a different number of neurons classified as invariant. We expanded on our initial findings and studied the effect of threshold value on the number of invariant neurons during training. As expected, a higher threshold value leads to a higher percentage of invariant neurons. The table below presents the percentage of invariant neurons observed at different threshold values, and the overall training accuracy of the FEMNIST model, using a sub-model size of 0.75 for the stragglers.

Table 3: Threshold vs accuracy results

Threshold value (%)	Percentage of Invariant Neurons (%)	Accuracy (%)
1	3	80.1
3	6	80.3
5	13	80.45
7	18	80.65
8	22	80.7
10	31	80.5

We observe that to obtain the desired accuracy and mitigate performance bottlenecks of stragglers, it is critical to choose the threshold that has the closest number of invariant neurons as the number of neurons to be dropped for the sub-model. The FLuID framework can automatically tune the threshold for the desired model based on the straggler performance, as described in Section 5.

A.3 Impact of Sub-Model Size on Training Time

In this section, we present evidence that there is a linear relationship between client training time and sub-model size. We evaluated the training time of 5 Android-based mobile phones from 2018 to 2020 outlined in Table 1. The training time is expressed in the percentage of the training time for the

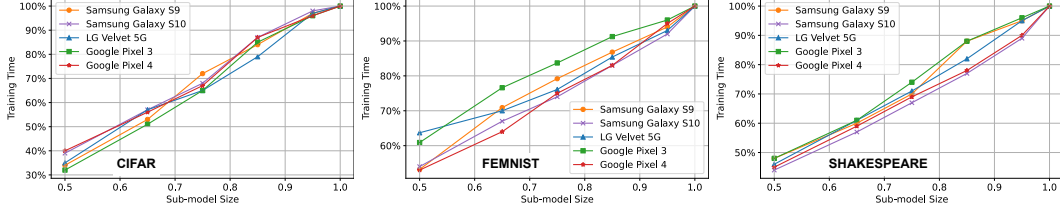


Figure 7: Linear relationship between training time and model size across all three datasets

full model size ($r = 1.0$). Across CIFAR10, FEMNIST, and Shakespeare, the training time of all five mobile clients decreases linearly as the sub-model size decreases and falls within 10% of the sub-model size. Using this insight, FLuID selects a sub-model size r as the available sub-model, the size that's closest to the inverse of *Speedup*.

A.4 Additional Experiments with Scalability Studies.

In this section, we show that in the case that the network has multiple stragglers, FLuID does not assume that all stragglers have similar capabilities or select a sub-model for all stragglers based on the slowest device. FLuID can select sub-model sizes for each straggler client based on each client's own capabilities. In this experiment, we cluster devices of similar capabilities into four groups of sub-model sizes. Table 4 presents the accuracy when stragglers are assigned to 4 equal-sized clusters (sub-model size 0.65, 0.75, 0.85, 0.95). The overall accuracy generally lies between assigning sub-model sizes of 0.75 and 0.85 for all stragglers. This way, FLuID can achieve a higher training accuracy with a shorter training time, even with stragglers that are initially more than 35% slower than non-straggler devices.

Table 4: Accuracy comparison of Random Dropout, Ordered Dropout, and Invariant Dropout as we cluster stragglers into different sub-model size groups.

	Random	Ordered	Invariant
CIFAR10	71.7	72.3	72.7
FEMNIST	77.5	77.4	78.2
Shakespeare	53.8	53.9	54.1

A.5 Additional Experiments with Varying Straggler Percentage.

In this section, we show that FLuID is capable of handling multiple ratios of stragglers. We have run additional experiments to explore the impact of different ratios of stragglers. One common trend we observed across state-of-the-art techniques and FLuID is that accuracy decreases as the ratio of stragglers is increased as more of the devices are now being trained only on the sub-model. Nonetheless, in all the cases, Invariant Dropout offers the highest accuracy because it is aware of the neuron gradient changes and only drops the least changing neurons. The accuracy results of varying the straggler ratios while using 0.75-sized sub-models are summarized in Figure 8.

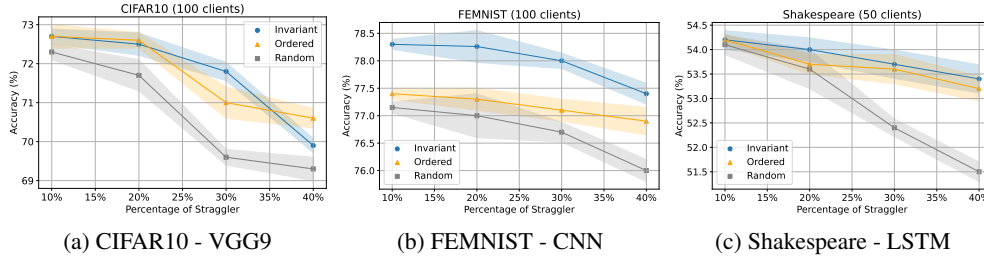


Figure 8: Accuracy of varying the straggler ratios from 10% to 40% with 0.75 sub-model size